ACM Symposium on Solid Modeling and Applications (2004)
G. Elber, N. Patrikalakis, P. Brunet (Editors)

Stability and homotopy of a subset of the medial axis

F. Chazal † and A. Lieutier ‡

Abstract

Medial Axis is known to be unstable for non smooth objects. For an open set $\mathcal{O}$, we define the Weak Feature Size, wfs, *minimum distance between $\mathcal{O}^c$ and the critical points of the function distance to $\mathcal{O}^c$. We introduce the* "Lambda-Medial Axis" *of $\mathcal{O}$, $\mathcal{M}_\lambda$, a subset of the Medial Axis of $\mathcal{O}$ which captures the Homotopy type of $\mathcal{O}$ when $\lambda <$* wfs. *We show that, at least for some "regular" values of λ, $\mathcal{M}_\lambda$ remains stable under Hausdorff distance perturbations of $\mathcal{O}^c$.*

1. Introduction and related works

The Medial Axis $\mathcal{M}$ of an open set $\mathcal{O}$ in $\mathbb{R}^n$ is the set of points $x \in \mathcal{O}$ for which there is at least 2 closest points on the complement $\mathcal{O}^c$ (see section 2). The Medial Axis has applications in image analysis and mathematical morphology [18], Solid Modeling [4], or domain decomposition for CAD to CAE (i.e. Finite Elements) models generation [20, 21].

For a few years, most successfull methods for reconstructing a 3D shape from unorganised data points sampled on the shape boundary start with a 3-dimensional Voronoi Diagram of the points [3, 5, 12, 5, 2, 1]. Recall that, for a finite set of points S, the Medial Axis of the complement S^c of S is the Voronoi Diagram of S, or, more accurately, the union of the cells of dimension at most $n-1$ in the Voronoi Diagram. In the "Power Crust" paper [2], the proposed reconstruction algorithm consists in:

1. computing an approximation of the Medial Axis of the shape from the Voronoi Diagram of the sampled points,
2. reconstructing the Solid corresponding to this approximate Medial Axis, together with the associated distance function.

The approximation of the Medial Axis in step 1) consists in the selection of a subset of the Voronoi vertices, called the poles. It has been shown in [5] and [2] that, for a C^2 smooth surface, the set of poles converges toward the Medial Axis in Hausdorff distance when the sampling density approaches 0. Even if this is not explicit in other algorithms based on a 3D Voronoi diagram, topological fidelity in reconstruction algorithms is related to the ability to select a relevant subset of the Voronoi Diagram of the sampling that approaches the Medial Axis of the underlying object.

The exact computation paradigm assumes exact inputs belonging to countable sets, for which usual geometric predicates are decidable and can then be computed exactly. On the other hand considering approximate inputs (or inputs belonging to uncountable sets) asks for a model of computation in which the continuity (that is the stabiliy) of the operator is required: one should be able to compute an arbitrary accurate appoximation of the output using a sufficiently accurate approximation of the input. Proposed algorithms for the computation of the Medial axis in the first model of computation includes Voronoi Diagram of a finite set of rational points, and seams to be feasible for exact (that is rational or algebraic numbers) polyhedral inputs (see [13, 8]).

For non exact inputs, such as CAD BRep models or measured objects, one has to do with aproximation. Indeed, the computation of the Medial Axis of two-dimensional or three-dimensional solids is known to be problematic due to its unstability : small variations in the boundary of an object result in large variations of its Medial Axis. For example, if the input is a BRep solid, an arbitrary small G^0 (incidence) or G^1 (tangency) discontinuity between two boundary elements entails a large "spike" in the Medial Axis. We would like to emphasize here that this unstability is not a technical difficulty related to a specific algorithm: when the output is not a continuous function of the input, the result of any computation is meaningless, unless assuming "exact" input datas, which is not realistic for measured or even usual CAD datas. Following the ideas developped for surface reconstruction algorithms, some authors have examined how a specific subset of the Voronoi complex of the sampled points can be used as an approximation of the Medial axis [2, 9, 10]. These approaches assumes that the sampled points lie *exactely* on a smooth surface with a positive lfs. The lfs is the minimal distance from the boundary to the Medial Axis and gives an upper bound on the curvature for a C^2 surface. Indeed, in order to approximate the Medial Axis with respect to the Hausdorff distance, one needs informations about the boundary both in position, tangency and curvature (see [7]). These informations are in a sense hidden in the assumptions of positive lfs and exact sampling. However, regarding the sampling informations actually available and the kind of solids encountered in real life, one should be able to achieve reasonable approximations with weaker assumptions. *The*

† Université de Bourgogne, Institut de Mathématiques de Bourgogne, UMR 5584 CNRS, (France), fchazal@u-bourgogne.fr
‡ Dassault Systèmes (Aix-en-Provence) and LMC/IMAG, Grenoble France

aim of this work is to understand what kind of approximation one can obtain with a priori minimum assumptions on the regularity of the solid boundary or on the quality of the sampling.

We consider a general class of objects (namely the open bounded subsets of $\mathbb{R}^n$) and we replace the notion of sampling by the more general class of closed sets approximating the boundary within a given Hausdorff distance. Practically, this point of view allows to consider noised sampling of non smooth objects. Of course, without any information on the existence of tangent planes or bounded curvature, one cannot expect to find a good Hausdorff distance approximation of the Medial Axis. Instead, we are looking to another object, $\mathcal{M}_\lambda$, subset of the Medial Axis. $\mathcal{M}_\lambda$ *is the set of points for which any ball containing the set of closest points on the boundary has radius at least* λ.

Beyond the Medial Axis, the distance function to the complement induces in fact a finer structure. In [17], the Homotopy equivalence of any open bounded subset of $\mathbb{R}^n$ with its Medial Axis has been proved using a continuous deformation flow. This flow integrates, in some weakened sense , a discontinuous vector field ∇ which is an extension of the gradient of the distance function. Intuitively, for a point $x \in \mathcal{O}$, $\nabla(x)$ gives the local direction to go in order to optimally increase the distance to the complement, while its norm is the rate of growth of this distance when moving in this direction (see section 2). This flow has been independently introduced in [12, 16, 11] in the particular situation where the complement $\mathcal{O}^c$ of $\mathcal{O}$ is finite (i.e. for Voronoi Diagrams). These authors have shown that the Flow Diagram induces a nice structure on the Voronoi Diagram. According to [17], this flow and the associated structures remain valid for general open sets. These structures rely in particular on the *critical points* of this flow, that is the set of points x for which $\nabla(x) = 0$, as well as the stable/unstable manifolds [12, 16] associated to these critical points.

We introduce the Weak Feature Size, wfs, minimum distance between $\mathcal{O}^c$ and the critical points of $\mathcal{O}$. We show in section 3 that performing an erosion of distance d on $\mathcal{O}$, that is removing from $\mathcal{O}$ any point at distance at most d from $\mathcal{O}^c$, preserves the homotopy type of $\mathcal{O}$ as far as $d <$ wfs. $\mathcal{M}_\lambda$ enjoys the property of capturing the Homotopy type of the object when $\lambda <$ wfs and, when $\lambda >$ wfs its homotopy corresponds to a filtered homotopy that ignores topological features smaller than λ (section 3).

We claim that $\mathcal{M}_\lambda$ is more relevant than $\mathcal{M}$ in most practical situations because it remains stable and well defined without any assumption on the smoothness of the object or of an unlikely exactness of the sampling. Section 5 examines in which precise sense the $\mathcal{M}_\lambda$ of the "exact object" can be approximated from the $\mathcal{M}_\lambda$ of its Hausdorff approximation, therefore giving a sound foundation of any computation of this object in realistic situations, which is proved hopeless for the Medial Axis. It also gives a straigh forward algorithm using filtered Voronoi diagrams of sampled points as approximations (see section 5.1) We chose to keep the proofs that are related to the geometry of $\mathcal{M}_\lambda$ and ommit some long proofs related to real analysis issue. The missing proofs can be found in [6].

2. Definitions

2.1. The continuous deformation $\mathfrak{C}$

We use the following definitions and notations. In the whole paper, $\mathcal{O}$ and $\mathcal{M}$ always denote respectively a bounded open subset of $\mathbb{R}^n$ and its Medial Axis defined below. For any set X, $\overline{X}$, X°, ∂X and X^c denote respectively the closure, the interior, the boundary and the complement of X. $\mathbb{B}_{x,r}$ and $\mathbb{B}^\circ_{x,r}$ respectively denote the closed and open ball of center x and radius r in $\mathbb{R}^n$.

For any point $x \in \mathcal{O}$, we denote by $\Gamma(x)$ the set of closest boundary points, that is :

$$\Gamma(x) = \{y \in \mathcal{O}^c,\ d(x,y) = d(x,\mathcal{O}^c)\} = \{y \in \partial\mathcal{O},\ d(x,y) = d(x,\partial\mathcal{O})\}$$

Because $\partial\mathcal{O}$ is compact, $\Gamma(x)$ is a non empty compact set. For a set E, $|E|$ denotes the cardinal of E.

Definition 2.1 (Medial Axis) The Medial Axis $\mathcal{M}$ of the open set $\mathcal{O}$ is the set of points x of $\mathcal{O}$ who have at least 2 closest boundary points :

$$\mathcal{M} = \{x \in \mathcal{O},\ |\Gamma(x)| \geq 2\}$$

The strictly positive, real valued function $\mathcal{R}$ defined on $\mathcal{O}$ is the distance to the boundary:$\mathcal{R}(x) = d(x,\mathcal{O}^c)$. One can check, using the triangular inequality twice, that $\mathcal{R}$ is 1-Lipschitz.

There always exists a unique closed ball with minimal radius enclosing $\Gamma(x)$. The real valued, positive function $\mathcal{F}$ is defined as the radius of this smallest closed ball enclosing $\Gamma(x)$. (cf. figure 1). In other words $\mathcal{F}(x) = \inf\{r, \exists y \in \mathbb{R}^n, \mathbb{B}_{y,r} \supset \Gamma(x)\}$. One proves in [17] that $\mathcal{F}$ is *upper semicontinuous*, that is :

$$\forall \varepsilon \in \mathbb{R},\quad \{x \in \mathcal{O}, \mathcal{F}(x) < \varepsilon\} \text{ is open}$$

Similarly, $\Theta(x)$ denotes the center of this smallest enclosing ball. Of course, when $x \notin \mathcal{M}$, we have $\Gamma(x) = \{\Theta(x)\}$ and $\mathcal{F}(x) = 0$.

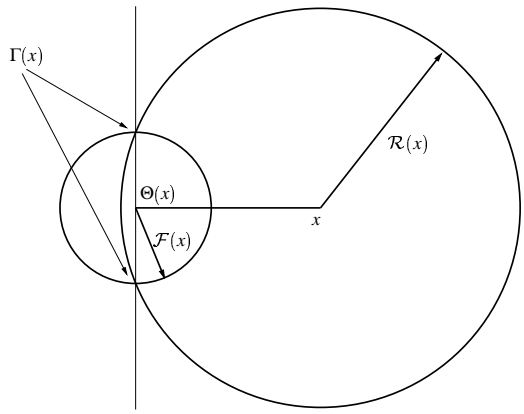

Figure 1: *A 2-dimensional example with 2 closest points*

The vector function ∇ extends the gradient of $\mathcal{R}$. $\nabla(x)$ is defined for all $x \in \mathcal{O}$ and coincides with the gradient of $\mathcal{R}$ when $x \in \mathcal{O} - \overline{\mathcal{M}}$. It is defined as follows:

$$\nabla(x) = \frac{x - \Theta(x)}{\mathcal{R}(x)}$$

One has the following relation (see [17]):

$$\nabla(x)^2 = 1 - \frac{\mathcal{F}(x)^2}{\mathcal{R}(x)^2} \tag{1}$$

The map $x \mapsto \|\nabla(x)\|$ is lower semicontinuous (see [17]). The *critical points* of ∇ are the points x for which $\nabla(x) = 0$. When $\mathcal{O}^c$ is

finite, that is for Voronoi Diagrams, critical points are the intersections of the Delaunay cells with their dual Voronoi cell (when they do intersect). In the general case, a point x is a critical point if and only if it lies in the convex hull of $\Gamma(x) : x \in \mathcal{CH}(\Gamma(x))$.

∇ is not continuous. However, it is shown in [17] that Euler schemes using this vector fields converges uniformly, when the integration step decreases, toward a continuous flow $\mathfrak{C} : \mathbb{R}^+ \times \mathcal{O} \mapsto \mathcal{O}$. This flow realizes the homotopy equivalence (see section 2.2) between $\mathcal{O}$ and $\mathcal{M}$.

One proves in [17] the following equalities:

$$\mathfrak{C}(t,x) = x + \int_0^t \nabla(\mathfrak{C}(\tau,x))d\tau \tag{2}$$

$$\mathcal{R}(\mathfrak{C}(t,x)) = \mathcal{R}(x) + \int_0^t \nabla(\mathfrak{C}(\tau,x))^2 d\tau \tag{3}$$

The curve image of $t \mapsto \mathfrak{C}(t,x)$ is rectifiable and its arc length is an increasing function of t given by:

$$s(t) = \int_0^t \|\nabla(\mathfrak{C}(\tau,x))\|d\tau \tag{4}$$

and, if one denotes $s \mapsto t(s)$ the inverse map:

$$\mathcal{R}(\mathfrak{C}(t(s),x)) = \mathcal{R}(x) + \int_0^s \|\nabla(\mathfrak{C}(t(\sigma),x))\|d\sigma \tag{5}$$

The main object studied in the paper, $\mathcal{M}_\lambda$ is defined by $\mathcal{M}_\lambda = \{x \in \mathcal{O}, \mathcal{F}(x) \geq \lambda\}$. Notice that, because $\mathcal{F}$ is upper semicontinuous $\mathcal{M}_\lambda$ is a closed set.

2.2. homotopy equivalence

Two maps $f_0 : X \mapsto Y$, and $f_1 : X \mapsto Y$, are said *homotopic* if there is a continuous map H, $H : [0,1] \times X \mapsto Y$, such that $\forall x \in X, H(0,x) = f_0(x)$ and $H(1,x) = f_1(x)$.

The homotopy equivalence between topological sets enforces a one-to-one correspondance between connected components, cycles, holes, tunnels, cavities, or higher dimensional topological features of the two sets, as well as the way these features are related.

The definition of homotopy equivalence can be found in [15] pages 171-172 or [19] pages 108:

Two spaces X and Y are said to have the same homotopy type if there are continuous maps $f : X \mapsto Y$ and $g : Y \mapsto X$ such that $g \circ f$ is homotopic to the identity map of X and $f \circ g$ is homotopic to the identity map of Y.

We are in the case where $Y \subset X$ and g is the canonical inclusion:$\forall y \in Y, g(y) = y$. In section 3, as in [17], the homotopy equivalence is proved using the following characterization.

Proposition 2.2 If $Y \subset X$ and there exists a continuous map H, $H : [0,1] \times X \mapsto X$ such that:

- $\forall x \in X, H(0,x) = x$
- $\forall x \in X, H(1,x) \in Y$
- $\forall y \in Y, \forall t \in [0,1], H(t,y) \in Y$

then, X and Y have same homotopy type.
If one replaces the third condition by: $\forall y \in Y, H(1,y) = y$, H defines a *deformation retract* of X towards Y.

3. Homotopy type of $\mathcal{M}_\lambda(\mathcal{O})$

The *Weak Feature Size*, denoted $\text{wfs}(\mathcal{O})$, of an open, bounded subset $\mathcal{O}$ of $\mathbb{R}^n$ is the distance between the complement $\mathcal{O}^c$ and the set of critical points $\{x \in \mathcal{O}, \nabla(x) = 0\}$ of the distance function. In this section, we show that, if $\lambda < \text{wfs}(\mathcal{O})$, then $\overline{\mathcal{O}_\lambda} = \{x \in \mathcal{O},\ \mathcal{R}(x) \geq \lambda\}$, is a deformation retract of $\mathcal{O}$ (theorem (3.6)) and that $\mathcal{M}_\lambda(\mathcal{O})$ carries the homotopy type of $\mathcal{O}$ (theorem (3.9)) .

3.1. Definition of $\mathbf{F}_\beta(\mathcal{O})$, $\mathbf{G}_\beta(\mathcal{O})$ and first properties:

We denote by $\mathcal{O}$ an open, bounded subset of $\mathbb{R}^n$. The set of critical points of the vector field ∇, $\{x \in \mathcal{O}, \nabla(x) = 0\}$, or, equivalently, the set of *fix points* of the map $x \mapsto \mathfrak{C}(t,x)$ will be denoted by $\mathbf{F}(\mathcal{O})$. More generally, we introduce the set $\mathbf{F}_\beta(\mathcal{O})$:

$$\mathbf{F}_\beta(\mathcal{O}) = \{x \in \mathcal{O}, \|\nabla(x)\| \leq \beta\}$$

With this notation, one has of course $\mathbf{F}_0(\mathcal{O}) = \mathbf{F}(\mathcal{O})$. Because the map $x \mapsto \|\nabla(x)\|$ is lower semi-continuous, $\mathbf{F}_\beta(\mathcal{O})$ is a closed set for the relative topology in $\mathcal{O}$. One has of course $\beta \leq \beta' \Rightarrow \mathbf{F}_\beta(\mathcal{O}) \subset \mathbf{F}_{\beta'}(\mathcal{O})$. Notice that $\mathbf{F}_\beta(\mathcal{O})$ is related to the filtering of the Voronoi diagram by angle criterion, taking β as the cos of the angle [14]. However, when $\beta > 0$, $\mathbf{F}_\beta(\mathcal{O})$ is not, in general, globally invariant by the action of $x \mapsto \mathfrak{C}(t,x)$ and, therefore does not, in general, keep the homotopy type of $\mathcal{O}$.

We introduce now $\mathbf{G}_\beta(\mathcal{O})$, the *smallest superset of* $\mathbf{F}_\beta(\mathcal{O})$ *that is globally invariant by the action of* $x \mapsto \mathfrak{C}(t,x)$:

$$\mathbf{G}_\beta(\mathcal{O}) = \mathfrak{C}(\mathbb{R}^+, \mathbf{F}_\beta(\mathcal{O})) = \{x \in \mathcal{O}, \exists t \in \mathbb{R}^+, \exists y \in \mathbf{F}_\beta(\mathcal{O}), x = \mathfrak{C}(t,y)\}$$

One has of course $\mathbf{F}_\beta(\mathcal{O}) \subset \mathbf{G}_\beta(\mathcal{O})$ and $\beta \leq \beta' \Rightarrow \mathbf{G}_\beta(\mathcal{O}) \subset \mathbf{G}_{\beta'}(\mathcal{O})$. Unlike $\mathbf{F}_\beta(\mathcal{O})$, $\mathbf{G}_\beta(\mathcal{O})$ carries the homotopy of $\mathcal{O}$, as stated in the Lemma 3.2 below.

Lemma 3.1 Let D be the diameter of $\mathcal{O}$.

$$\forall x \in \mathcal{O}, \mathfrak{C}\left(\frac{D}{\beta^2}, x\right) \in \mathbf{G}_\beta(\mathcal{O})$$

The proof of the Lemma is a direct application of equality (3) and can be found in [6].

Lemma 3.2 For any $\beta > 0$, $\mathbf{G}_\beta(\mathcal{O})$ has the same homotopy type than $\mathcal{O}$.

Proof We use the characterization of proposition 2.2. From the definition of $\mathbf{G}_\beta(\mathcal{O})$, it is clear that it is globaly invariant by the action of $x \mapsto \mathfrak{C}(t,x)$, that is :

$$\forall x \in \mathbf{G}_\beta(\mathcal{O}), \forall t \in \mathbb{R}^+, \mathfrak{C}(t,x) \in \mathbf{G}_\beta(\mathcal{O})$$

From this property and lemma 3.1, the homotopy $[0,1] \times \mathcal{O} \mapsto \mathcal{O}$ defined by $(t,x) \mapsto \mathfrak{C}(t\frac{D}{\beta^2}, x)$ defines an homotopy equivalence between $\mathcal{O}$ and $\mathbf{G}_\beta(\mathcal{O})$. □

3.2. Introduction of the Weak Feature Size (wfs)

For two sets A, B we denotes by $d(A,B)$ the minimum distance between all the pairs of points in A and B: $d(A,B) = \inf_{a \in A, b \in B} d(a,b)$

Definition 3.3 We call *Weak Feature Size* of $\mathcal{O}$, denoted by $\text{wfs}(\mathcal{O})$, the distance between $\mathcal{O}^c$ and $\mathbf{F}(\mathcal{O})$:

$$\text{wfs}(\mathcal{O}) = \inf_{x \in \mathbf{F}(\mathcal{O})} \mathcal{R}(x)$$

Notice that, unlike the usual Local Feature Size (lfs), wfs may be positive for non smooth objects. In particular it is positive for sets with peacewise linear boundary.

For $\varepsilon > 0$ and a set X, one denotes by $X^{+\varepsilon}$ the open set of points whose distance to X is strictly smaller than ε. The proof of the Lemma below can be found in [6]:

Lemma 3.4

$$\forall \varepsilon > 0, \ \ \exists \beta > 0, \ \ \mathbf{F}_\beta(\mathcal{O}) \subset \left(\mathcal{O}^c\right)^{+\varepsilon} \cup \mathbf{F}(\mathcal{O})^{+\varepsilon}$$

Let us denote by $\mathbf{D}_\varepsilon$ the set of points of $\mathcal{O}$ whose distance to the complement $(\mathcal{O}^c)$ is comprised between ε and $wfs - \varepsilon$:

$$\mathbf{D}_\varepsilon = \{x \in \mathcal{O}, \varepsilon \leq \mathcal{R}(x) \leq wfs - \varepsilon\}$$

From lemma 3.4, we know that, for any $\varepsilon > 0$ there exists $\beta > 0$ such that

$$\forall x \in \mathbf{D}_\varepsilon, \ \ \beta < \|\nabla(x)\| \leq 1 \tag{6}$$

Let x in $\mathbf{D}_\varepsilon$ and $r \in [0, wfs - \varepsilon - \mathcal{R}(x)]$. From equation (3) and (6), there exists a unique t, $t \in \left[0, \frac{wfs}{\beta^2}\right]$ such that:

$$\mathcal{R}(\mathfrak{C}(t,x)) = \mathcal{R}(x) + r$$

This allows to introduce the map $\mathfrak{C}_r(r,x) = \mathfrak{C}(t,x)$ defined for any $x \in \mathbf{D}_\varepsilon$ and $r \in [0, wfs - \varepsilon - \mathcal{R}(x)]$. This means that, for $x \in \mathbf{D}_\varepsilon$ and as far as the distance to $\mathcal{O}^c$ is less than $wfs - \varepsilon$, one can parametrize the trajectory of x by the distance r to the complement.

The lemma below ([6]), states that $\mathfrak{C}_r$ is Lipschitz with respect to both variables.

Lemma 3.5 For any $\varepsilon > 0$, using again the β of lemma 3.4, one has:

$$\forall x_1, x_2 \in \mathbf{D}_\varepsilon, \ \ \forall r_1 \in [0, wfs - \varepsilon - \mathcal{R}(x_1)], \ \ \forall r_2 \in [0, wfs - \varepsilon - \mathcal{R}(x_2)]$$

$$\|\mathfrak{C}_r(r_2, x_2) - \mathfrak{C}_r(r_1, x_1)\| \leq \frac{1}{\beta}|r_2 - r_1| + \left(\left(1 + \frac{1}{\beta}\right) e^{\frac{wfs}{\varepsilon\beta^2}} + \frac{1}{\beta}\right) \|x_2 - x_1\|$$

Following [17], we denote by $\mathcal{O}_d$ the set of points of $\mathcal{O}$ at distance greater than d from the boundary:

$$\mathcal{O}_d = \{x \in \mathcal{O}, \mathcal{R}(x) > d\}$$

and by $\overline{\mathcal{O}_d}$ the closure of $\mathcal{O}_d$

Theorem 3.6 if $d < \text{wfs}(\mathcal{O})$, $\overline{\mathcal{O}_d}$ is a deformation retract of $\mathcal{O}$ and $\mathcal{O}_d$ has the homotopy type of $\mathcal{O}$.

Proof Proposition 2.2 gives the definition of a deformation retract. Assuming $d < \text{wfs}(\mathcal{O})$, we define the map H_d:

$$\begin{aligned} H_d : [0,1] \times \mathcal{O} &\mapsto \mathcal{O} \\ (t,x) \mapsto H_d(t,x) &= \mathfrak{C}_r\left(t\left(d - \mathcal{R}(x)\right), x\right) \ \text{ if } \ \mathcal{R}(x) \leq d \\ &= x \ \text{ if } \ \mathcal{R}(x) \geq d \end{aligned}$$

H_d is a deformation retract of $\mathcal{O}$ toward $\overline{\mathcal{O}_d}$. Let $\varepsilon = \frac{\text{wfs} - d}{2}$. The map $H_{d+\varepsilon}$ defines the homotopy equivalence of $\mathcal{O}$ toward $\mathcal{O}_d$ using the characterization given in Proposition 2.2. □

We define $\mathbf{G}^d_\beta(\mathcal{O})$, the *smallest superset of* $\mathcal{O}_d \cap \mathbf{F}_\beta(\mathcal{O})$ *that is globally invariant by the action of* $x \mapsto \mathfrak{C}(t,x)$:

$$\begin{aligned} \mathbf{G}^d_\beta(\mathcal{O}) &= \mathfrak{C}(\mathbb{R}^+, \mathcal{O}_d \cap \mathbf{F}_\beta(\mathcal{O})) \\ &= \{x \in \mathcal{O}, \exists t \in \mathbb{R}^+, \exists y \in \mathcal{O}_d \cap \mathbf{F}_\beta(\mathcal{O}), x = \mathfrak{C}(t,y)\} \end{aligned}$$

Lemma 3.7 if $d < \text{wfs}(\mathcal{O})$ and $\beta > 0$, $\mathbf{G}^d_\beta$ has the homotopy type of $\mathcal{O}$.

Proof We use once again the characterization given in Proposition 2.2. One has trivially $\mathbf{G}^d_\beta \subset \overline{\mathcal{O}_d}$. Using lemma 3.1 one gets the homotopy equivalence with $\overline{\mathcal{O}_d}$ using the homotopy $[0,1] \times \overline{\mathcal{O}_d} \mapsto \overline{\mathcal{O}_d}$ defined by $(t,x) \mapsto \mathfrak{C}\left(t\left(\frac{D}{\beta^2}\right), x\right)$. This together with theorem 3.6 gives the result. □

3.3. Homotopy type of $\mathcal{M}_\lambda(\mathcal{O})$

Lemma 3.8 If $\lambda < \text{wfs}(\mathcal{O})$, then there exists $\beta > 0$ such that

$$\mathbf{G}^\lambda_\beta \subset \mathcal{M}_\lambda(\mathcal{O})$$

Proof The proof is ommitted in this short version (see [6]). □

Theorem 3.9 If $\lambda < \text{wfs}(\mathcal{O})$, $\mathcal{M}_\lambda(\mathcal{O})$ has the homotopy type of $\mathcal{O}$.

Proof We use once again the characterization given in Proposition 2.2. Because the map $t \mapsto \mathcal{F}(\mathfrak{C}(t,x))$ is increasing and from the definition of $\mathcal{M}_\lambda(\mathcal{O})$ it is clear that

$$\forall x \in \mathcal{M}_\lambda(\mathcal{O}), \forall t \in \mathbb{R}^+, \mathfrak{C}(t,x) \in \mathcal{M}_\lambda(\mathcal{O})$$

With the value of β taken from lemma 3.8 and using lemma 3.1 again, one get that the map $[0,1] \times \mathcal{M}_\lambda(\mathcal{O}) \mapsto \mathcal{M}_\lambda(\mathcal{O})$ defined by $(t,x) \mapsto \mathfrak{C}\left(t\frac{D}{\beta^2}, x\right)$ defines an homotopy equivalence between $\mathcal{M}_\lambda(\mathcal{O})$ and $\mathbf{G}^d_\beta$. This, together with lemma 3.7, proves the theorem. □

4. Stability of $\mathcal{M}_\lambda$ under perturbations

Let $\mathcal{O}$ be an open bounded subset of $\mathbb{R}^n$, let $D = \sup_{(x,y)\in\mathcal{O}} d(x,y)$ be its diameter and let $\lambda > 0$ be a fixed real number. In this section we prove that the λ-medial axis of $\mathcal{O}$ satisfies some stability properties when one makes a small perturbation of $\mathcal{O}$ (for Hausdorff distance). The results of this section are used to give a robust approximation algorithm in next section.

Theorem 4.1 Let $\varepsilon > 0$ be such that $10\varepsilon < \lambda$. For any bounded open set $\tilde{\mathcal{O}}$ such that $d_H(\mathcal{O}^c, \tilde{\mathcal{O}}^c) < \varepsilon$, for any $x \in \mathcal{M}_\lambda(\tilde{\mathcal{O}})$ and for any $\lambda' > 0$ such that $\lambda'^2 < \lambda^2 - 150\sqrt{\varepsilon}D^{3/2}$ and $\lambda' < \lambda - \varepsilon$, there exists a point $y \in \mathcal{M}_{\lambda'}(\mathcal{O})$ such that

$$d(x,y) \leq 2\sqrt{D}\sqrt{\varepsilon}.$$

The idea of the proof is to show that if $y(s)$ is the trajectory of the vector field ∇ issued from x, then it cannot remain during a long time outside of some $\mathcal{M}_{\lambda'}(\mathcal{O})$ for a well chosen value of λ'.

Proof From now on, one fixes a real $\varepsilon > 0$ and an open set $\tilde{\mathcal{O}}$ satisfying the hypothesis of the theorem. The notations $\tilde{\mathcal{R}}$, $\tilde{\mathcal{F}}$, $\tilde{\nabla}$ will respectively denote the distance function, the minimum radius function and the "gradient" vector field associated to $\tilde{\mathcal{O}}$. Let $x \in \mathcal{M}_\lambda(\tilde{\mathcal{O}})$. The functions $\mathcal{R}$ and $\tilde{\mathcal{R}}$ are related by

$$\mathcal{R}(x) - \varepsilon \leq \tilde{\mathcal{R}}(x) \leq \mathcal{R}(x) + \varepsilon. \tag{7}$$

Case $\nabla(x) = 0$**:** From previous inequalities one has $\mathcal{R}(x) \geq \lambda - \varepsilon$. It follows that if $\nabla(x) = 0$, then $\mathcal{R}(x) = \mathcal{F}(x) \geq \lambda - \varepsilon$ and x belongs to $\mathcal{M}_{\lambda'}(\mathcal{O})$ for any $\lambda' < \lambda - \varepsilon$.
Case $\nabla(x) \neq 0$**:** Let $y(s)$ be the "trajectory" of point x for vector field ∇ parametrized by arc-length and such that $y(0) = x$. While

$y(s)$ remains in the complementary of $\mathcal{M}_{\lambda'}(\mathcal{O})$ for some $\lambda' < \lambda - \varepsilon$, one has

$$\frac{d\mathcal{R}}{ds}(y(s)) = \|\nabla(y(s))\| \geq \sqrt{1 - \frac{\lambda'^2}{\mathcal{R}(y(s))^2}}.$$

Thus using the fact that $\mathcal{R}(.)$ is increasing along trajectories of ∇ it follows

$$\mathcal{R}^2(x) + 2s\sqrt{\mathcal{R}^2(x) - \lambda'^2} \leq \mathcal{R}^2(y(s)). \tag{8}$$

Denote by $\tilde{\Gamma}(x) = \{y \in \tilde{\mathcal{O}}^c : d(x,y) = d(x,\tilde{\mathcal{O}}^c)\} \subset \tilde{\mathcal{O}}^c$ the set of closest boundary points and denote by $\tilde{B}$ the smallest ball containing this set. Its radius is equal to $\tilde{\mathcal{F}}(x) \geq \lambda$. Let C be the cone of apex x constructed on the $(n-2)$-sphere $\tilde{S} = \mathbb{S}_{x,\tilde{\mathcal{R}}(x)} \cap \partial\tilde{B}$ and let $2\alpha_1$ be its apex angle (see figure 2).

Lemma 4.1 Angle α_1 satisfies the following inequation

$$2(\mathcal{R}(x) - \varepsilon)^2(2\cos^2\alpha_1 - 1) \leq 2(\mathcal{R}(x) + \varepsilon)^2 - 4\lambda^2. \tag{9}$$

Proof It follows from inequality (7) and classical relation between the edges of a triangle. See [6] □

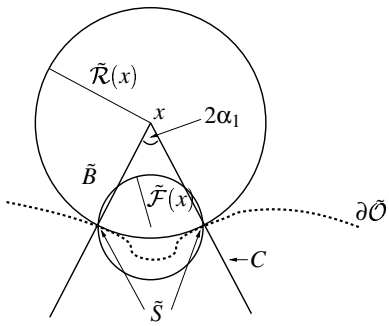

Figure 2:

Lemma 4.2 The distance $\mathcal{R}(y(s))$ between $y(s)$ and $\partial\mathcal{O}$ satisfies

$$\mathcal{R}(y(s))^2 \leq \left(\varepsilon + \sqrt{(\mathcal{R}(x)+\varepsilon)^2 + s^2 + 2s(\mathcal{R}(x)+\varepsilon)\cos\alpha_1}\right)^2. \tag{10}$$

Proof See [6] □

The end of the proof of theorem 4.1 will now follow from computations using inequalities (8), (9) and (10). Equation (8) forces $\mathcal{R}(y(s))$ to increase sufficiently fast while equation (10) forces increasing of $\mathcal{R}(y(s))$ to be sufficiently slow. Some quite long computations show that these two conditions cannot be simultaneously satisfied for a large range of values of s. In particular they cannot be satisfied for $s > 2\sqrt{R_0\varepsilon}$ which concludes the proof. All the computations are detailed in [6]. □

If one wants to estimate the distance of $\mathcal{M}_\lambda(\tilde{\mathcal{O}})$ to the medial axis $\mathcal{M}(\mathcal{O})$ one can deduce a better bound from previous proof.

Corollary 4.3 Let $\varepsilon > 0$ such that $\varepsilon < \min(\frac{\lambda}{10}, \frac{\lambda^3}{50D^2}, \frac{\lambda^4}{1200D^4})$. For any bounded open set $\tilde{\mathcal{O}}$ such that $d_H(\mathcal{O}^c, \tilde{\mathcal{O}}^c) < \varepsilon$, for any $x \in \mathcal{M}_\lambda(\tilde{\mathcal{O}})$ there exists a point $y \in \mathcal{M}(\mathcal{O})$ such that

$$d(x,y) \leq \frac{72D^2}{\lambda^2}\varepsilon.$$

5. Approximation of $\mathcal{M}_\lambda$ from a noisy sample of points

Results of previous section lead to an algorithm to approximate the λ medial axis of an open set $\mathcal{O}$ from the Voronoi diagram of a set of points sampled on the boundary of $\mathcal{O}$. The main interest of this algorithm is twofold. First, no hypothesis on the smoothness of the boundary of $\mathcal{O}$ is needed. Second, noisy samples are allowed, i.e. it is only required that the Hausdorff distance between $\partial\mathcal{O}$ and the sample is bounded by ε.

5.1. Computation of the λ-medial axis of a sample of points

Let $\mathcal{O}$ be a bounded open subset of $\mathbb{R}^n$ which boundary is denoted by $S = \partial\mathcal{O} = \mathcal{O}^c \cap \overline{\mathcal{O}}$.

Definition 5.1 A finite sample of points $\mathcal{E}$ such that the Hausdorff distance between S and $\mathcal{E}$ is less than ε is called an ε-*noisy sample* of S.

Let $\mathcal{E}$ be an ε-noisy sample and let $\tilde{\mathcal{O}}$ be the open set which is the complementary of $\mathcal{E}$ intersected with $\mathcal{O}^{+\varepsilon} = \{x \in \mathbb{R}^n : d(x,\mathcal{O}) < \varepsilon\}$ (see figure 3). Remark that $d_H(\mathcal{O}^c, \tilde{\mathcal{O}}^c) < \varepsilon$.

Lemma 5.2 If $\lambda > \varepsilon$, $\mathcal{M}_\lambda(\tilde{\mathcal{O}})$ is contained in the Voronoi diagram of $\mathcal{E}$.

Proof Let $x \in \mathcal{M}_\lambda(\tilde{\mathcal{O}})$ and suppose there exists $z \in (\mathcal{O}^{+\varepsilon})^c$ such that $d(x,z) = \tilde{\mathcal{R}}(x) > \varepsilon$. Thus the ball $\mathbb{B}_{x,\tilde{\mathcal{R}}(x)}$ is contained in $\mathcal{O}^{+\varepsilon}$ and does not contain any point of $\mathcal{E}$. Points x and z being in $\mathcal{O}$ and $(\mathcal{O}^{+\varepsilon})^c$ respectively, there exists a point y on the segment $[x,z]$ such that $y \in \partial O$. The ball $\mathbb{B}_{z,\varepsilon}$ does not intersect $\mathcal{O}$, so $d(y,z) \geq \varepsilon$ which entails $\mathbb{B}_{y,\varepsilon} \subset \mathbb{B}_{x,\tilde{\mathcal{R}}(x)}$. But $\mathbb{B}_{x,\tilde{\mathcal{R}}(x)} \cap \mathcal{E} = \emptyset$ and $d(y,\mathcal{E}) < \varepsilon$ because $d_H(\partial\mathcal{O}, \mathcal{E}) < \varepsilon$, which is a contradiction. Thus one has $\tilde{\Gamma}(x) \subset \mathcal{E}$. This concludes the proof. □

In the following $\mathcal{M}_\lambda(\tilde{\mathcal{O}})$ will be denoted $\mathcal{M}_\lambda(\mathcal{E})$ and one supposes that $\lambda > \varepsilon$. The "minimum radius function" $\mathcal{F}'$ associated to the open set $\mathbb{R}^n \setminus \mathcal{E}$ is constant on each cell of the Voronoi diagram of $\mathcal{E}$. It follows from previous lemma that $\mathcal{M}_\lambda(\mathcal{E})$ is the union of the cells of the Voronoi diagram of $\mathcal{E}$ on which $\mathcal{F}'$ is greater or equal to λ. So the following algorithm compute $\mathcal{M}_\lambda(\mathcal{E})$.

- $\mathcal{M}_\lambda(\mathcal{E}) = \emptyset$
- Compute Delaunay triangulation $\mathcal{D}$ of $\mathcal{E}$
- For each cell c of $\mathcal{D}$ do
  if c has smallest enclosing ball of radius greater than λ then $\mathcal{M}_\lambda(\mathcal{E}) = \mathcal{M}_\lambda(\mathcal{E}) \cup \text{dual}(c)$.

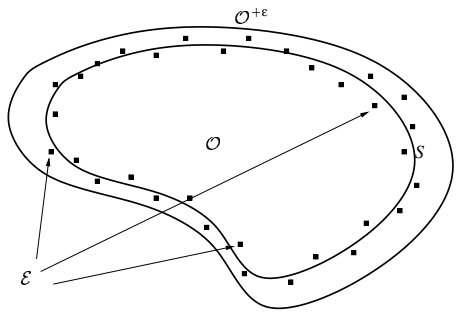

Figure 3:

5.2. Convergence of λ-medial axis

In order to be usefull, previous algorithm needs some convergence guarantees. That is one needs to know if the λ-medial axis of an ε-noisy sample of S converges to the λ-medial axis of $\mathcal{O}$ when ε goes to 0 (for the Hausdorff distance). This is not always the case for some values of λ as it is shown in the next example. Consider a cylinder C in $\mathbb{R}^3$ of radius $\lambda > 0$ and axis (Oz) bounding an open set $\mathcal{O}$. Then $\mathcal{M}_\lambda(\mathcal{O})$ is exactely the axis of C. But for any $\varepsilon > 0$, if one chooses a ε-noisy sample $\mathcal{E}$ of C on the cylinder of axis (Oz) and radius $\lambda - \varepsilon/2$, then $\mathcal{M}_\lambda(\mathcal{E}) = \emptyset$ (see figure 4). In some sense, such an example and such a value of λ are not "generic". The lack of convergence is due to the fact that $\mathcal{F}$ is equal to λ on a "big part" of the medial axis of $\mathcal{O}$, i.e. $\mathcal{F}$ is constant equal to λ on an open subset of $\mathcal{M}(\mathcal{O})$ for the induced topology on $\mathcal{M}(O)$. Recall from [17] p.71 that map $\mathcal{F}$ is upper semicontinuous and then since $\mathcal{O}$ is bounded, $\mathcal{M}_\lambda(\bar{\mathcal{O}})$ is a compact set for any $\lambda > 0$. Let $\mathcal{M}$ be the map from $]0;+\infty[$ to the set of compact subsets of $\mathcal{O}$, endowed with the topology induced by Hausdorff distance between compact sets, defined by $\mathcal{M}(\lambda) = \mathcal{M}_\lambda(\mathcal{O})$. Since $\mathcal{F}$ is upper continuous and since $\mathcal{M}(\lambda) \subseteq \mathcal{M}(\lambda')$ whenever $\lambda' < \lambda$, the map $\mathcal{M}$ is left continuous. This means that if λ_n is an increasing sequence which converges to some $\lambda > 0$, then $d_H(\mathcal{M}_{\lambda_n}(\mathcal{O}), \mathcal{M}_\lambda(\mathcal{O})) \to 0$ as $n \to 0$. The map $\mathcal{M}$ is continuous at λ if previous property is true for any sequence λ_n. Note that in above example $\mathcal{M}$ was not continuous at λ.

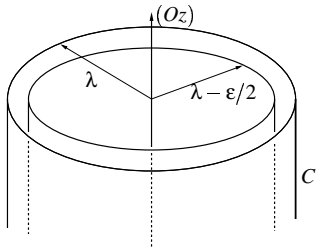

Figure 4:

On get the theorem below from theorem 4.1 and of some classical properties of Hausdorff topology on the set of compact sets in $\mathbb{R}^n$.

Theorem 5.1 Let $\mathcal{O}$ be an open bounded subset of $\mathbb{R}^n$ with boundary S and let $\lambda > 0$ be such that the above defined map $\mathcal{M}$ is continuous at λ. For any sequence $\mathcal{E}_n$ of ε_n-noisy samples of S satisfaying $\lim_{n\to+\infty} \varepsilon_n = 0$ one has

$$d_H(\mathcal{M}_\lambda(\mathcal{E}_n), \mathcal{M}_\lambda(\mathcal{O})) \longrightarrow 0 \quad \text{as} \quad n \to +\infty$$

References

[1] N. Amenta, S. Choi, T. Dey, N. Leekha *A simple algorithm for homeomorphic Surface Reconstruction.* International Journal of Computational Geometry and Applications Vol.12, No. 1,2(2002) pp.125-141 1

[2] N. Amenta, S. Choi, R. Kolluri *The Power Crust, unions of balls , the Medial Axis Transform* Computational:Theory and Applications, 2001 Vol.19:(2-3), pp.127-153 1

[3] N. Amenta, M. Bern *Surface Reconstruction by Voronoi Filtering* Discrete and Computational Geometry, no 22 pp.481-504(1999) 1

[4] R.Blanding, C.Brooking, M.Ganter , D.Storti *A skeletal-based solid editor* proceedings of the Fifth ACM Symposium on Solid Modeling and Applications (1999), pp.141-150 1

[5] J.D. Boissonnat, F. Cazals *Smooth surface reconstruction via natural neighbour interpolation of distance functions*. 16th ACM Symp. Computational Geometry (2000) pp.223-232 1

[6] F. Chazal, A. Lieutier, *Stability and homotopy of a subset of the medial axis*, Preprint Inst. Math. Bourgogne, CNRS UMR 5584, available at http://math.u-bourgogne.fr/topo/chazal/publications.htm 2, 3, 4, 5

[7] F. Chazal, R. Soufflet, *Stability and finiteness properties of medial axis and skeleton*, Journal of Dynamical and Control Systems, Vol. 10, No. 2, 149-170, 2004. 1

[8] T.Culver, J.Keyser, D.Manocha *Accurate Computation of the Medial Axis of a Polyhedron* proceedings of the Fifth ACM Symposium on Solid Modeling and Applications (1999), pp.179-190 1

[9] T. K. Dey, W. Zhao. *Approximate medial axis as a Voronoi subcomplex.* In 7th ACM Symposium on Solid Modeling and Applications, (2002) pages 356–366. 1

[10] T. K. Dey, W. Zhao *Approximating the medial axis from the Voronoi diagram with a convergence guarantee* Algorithmica, Vol. 38 (2004), 179–200. 1

[11] T. K. Dey, J. Giesen , M. John *Alpha-Shapes and Flow Shapes are Homotopy Equivalent.* Proc. 35rd Annual ACM Symposium on the Theory of Computing (STOC), (2003). 2

[12] H. Edelsbrunner *Surface reconstruction by wrapping finite point sets in space, in* Ricky Pollack and Eli Goodman Festschrift *ed. B. Aronov, S. Basu, J. Pach and M. Sharir*.

[13] M.Etzion, A.Rappoport *Computing the Voronoi Diagram of a 3-D Polyhedron by Separate Computation of its Symbolic and Geometric Parts* proceedings of the Fifth ACM Symposium on Solid Modeling and Applications (1999), pp.167-178 1, 2 1

[14] M.Foskey,M.C.Lin,D.Manocha *Efficient Computation of a Simplified Medial Axis,* proc. of the Eighth ACM Symposium on Solid Modeling and Applications (2003), pp.96-107 3

[15] W. Fulton. *Algebraic Topology, A First Course*. Graduate Texts in Mathematics. Springer-Verlag. 3

[16] J. Giesen , M. John, *The Flow Complex: A Data Structure for Geometric Modeling.* Proc. 14th Annual ACM-SIAM Symposium on Discrete Algorithms (SODA), (2003) 285-294. 2

[17] A. Lieutier, *Medial Axis Homotopy*, Proceedings of the Eighth ACM Symposium on Solid Modeling and Applications 2003. 2, 3, 4, 6

[18] G. Matheron. *Examples of Topological Properties of Skeletons* (Chapter 11), On the Negligibility of the Skeleton and the Absolute Continuity of Erosions (Chap 12), In Image Analysis and Math. Morphology, Volume 2: Theoretical Advances, Ed. by Jean Serra, pages 216–256. Academic Press, 1988.

[19] J. R.Munkres. *Elements of Algebraic Topology*. Addison-Wesley Publishing Company, 1984. 1 3

[20] A.Sheffer,M.Etzion,A.Rappoport, M. Bercovier *Hexahedral Mesh Generation using the Embedded Voronoi Graph* Proc, 7th International meshing Roundtable, Sandia National Lab, pp.347-364, Oct 1998 1

[21] K.Suresh *Automating the CAD/CAE Dimensional Reduction Process* proceedings of the Eighth ACM Symposium on Solid Modeling and Applications (2003), pp.76-85 1